VIBRATIONAL-ROTATIONAL TRANSITIONS IN AN $H_2 + F_2$ CHEMICAL LASER

G. G. DOLGOV-SAVEL'EV, V. F. ZHAROV, Yu. S. NEGANOV, and G. M. CHUMAK

Nuclear Physics Institute, Siberian Division, USSR Academy of Sciences

Experimental investigations of the time dependence of vibrational-rotational transitions in an $H_2 + F_2$ laser for various lengths of the initiating pulse ($\sim 10^{-8}$ sec and $\sim 10^{-5}$ sec) are described. It is shown that the use of an optical excitation pulse $\sim 10^{-8}$ sec long (second harmonic of a ruby laser) provides new possibilities of investigating the initial generation stage. The quantum yield (~ 200) of generation is measured in experiments with the second harmonic of the ruby laser. The mechanism of generation and the kinetics of chemical reactions proceeding in an $H_2 + F_2$ gas mixture are discussed.

THE basic properties of an $H_2 + F_2$ laser generating in the region of $3 \pm 0.2\ \mu$ were reported previously[1,2]. It was shown in[1-4] that population inversion is due to the chemical reaction of formation of an excited HF^* molecule. The study of the spectral composition of the emission and of the time dependence of individual transitions can provide an answer to some problems relating to the generation mechanism and the reaction kinetics in the gaseous mixture at the instant of generation.

In the experiments described below the reactions were initiated by photolysis of a fluorine molecule with different lengths of the initiating pulse τ_p. In one case we used flash lamps (pulse length 8 μsec), in another the second harmonic of a ruby laser generating a giant pulse with $\tau_p = 25$ nsec.

RESULTS OF EXPERIMENTS

1. In experiments with flash lamps we used a setup similar to that described in[1]. The initiating pulse was somewhat shorter and amounted to 3 μsec at the half-width (IFP-20000 lamps were used). To obtain the spectrum we used an IKM-1 monochromator with a diffraction grating of 200 lines/mm. The spectral width of the slit was 2 cm^{-1}. A GeAu crystal at liquid nitrogen temperature served as the detector. The total pressure of the $H_2 + F_2$ mixture was 24 mm Hg.

Figure 1 shows the initiating pulse and the spectrally unresolved generation pulse.

Figures 2b and 2c show typical oscilloscope traces of the emission from individual vibrational-rotational transitions. For some transitions, such as $P_{3-2}(8)$ and $P_{2-1}(11)$, the frequency difference was less than 2 cm^{-1} (Fig. 2a); in such a case they were identified by the time dependence of the trace intensity as compared for various positions of the Littrow mirror (Fig. 2a-c).

The table gives the frequency values of the observed vibrational-rotational transitions. The computation of transition frequencies was based on data published in[5].

Figure 3 shows the time dependence of the observed transition intensities averaged over several oscillograph traces.

Starting from a simple comparison of the obtained oscillograms, all generation times break down into three stages. In the first stage, 6 μsec long, we observe a rapid rise of generation and a fairly rapid
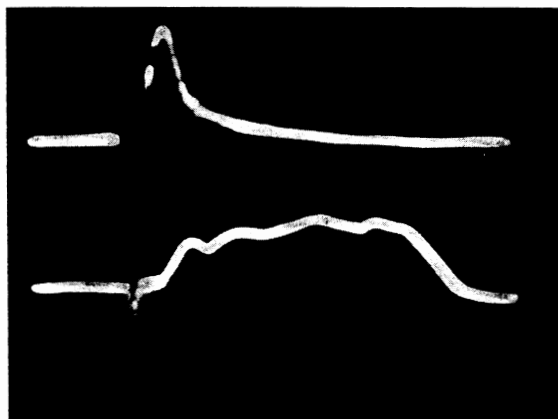

FIG. 1. Initiating pulse (top) and generation pulse (bottom). Total sweep duration 60 μsec.

nearly exponential drop of intensity of individual transitions (period I in Fig. 3). The duration of the individual transitions is 3—4 μsec. This period is associated with initiation of a reaction that results in the formation of a large number of free fluorine atoms. These react with a hydrogen molecule and form an excited molecule of hydrogen fluoride. After initiation is completed the system goes into the second stage (II in Fig. 3) during which the reaction $H + F_2 \rightarrow HF^* + F$ begins to "work" (transitions $v(3 \rightarrow 2)$, $v(4 \rightarrow 3)$, etc., appear). The duration of emission of individual transitions increases to 20 μsec. During this period (from 6 to 30 μsec from the beginning of generation) we observe a series of cascade transitions such as $P_{4-3}(7) \rightarrow P_{3-2}(8)$. The mixture temperature slowly rises.

The third generation stage (III in Fig. 3) is characterized by a sharp rise in the rotational temperature. The duration of transitions decreases to 5 μsec and generation terminates.

2. The experiments with generation in a mixture using a light-pulse length of 25 μsec were performed in the setup shown in Fig. 4. We used the second harmonic of a ruby laser operating in one of two modes: (1) free-running mode yielding a 10 J pulse 250 μsec long at the half width, and (2) Q-switched mode yielding a 1 J pulse 25 nsec long. The conversion to the second harmonic was accomplished with the aid of a potassium
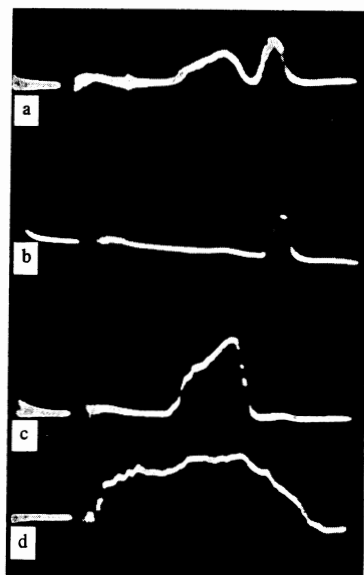
FIG. 2. Oscillograms of individual vibrational-rotational transitions ($\tau_p \sim 8$ μsec). a—unresolved transitions $P_{3-2}(8)$ and $P_{2-1}(11)$; b—transition $P_{2-1}(11)$; c—transition $P_{3-2}(8)$; d—total generation pulse. Total sweep duration 60 μsec.

dihydrophosphate crystal. An f = 100 cm lens ensured a 10% conversion of the ruby laser emission.

Emission at the fundamental frequency was blocked by a UFS-6 filter 5 mm thick, while the second harmonic emission was allowed to enter the working region through an opening in the resonator mirror.

The cell was fabricated from copper tubing 2 cm in diameter and 100 cm long fitted with CaF_2 windows at the Brewster angle. The cell and the feeding lines from the gas system were cooled with liquid nitrogen vapor down to $100-150°K$. The temperature was measured with a copper-constantan thermocouple. The above temperature allows for mixture pressures up to 100 mm Hg without explosion and with freedom from volatile fluoride impurities.

The emission beam was split off by a semitransparent quartz plate 1 mm thick for analysis. The input energy ($\lambda = 3470$ Å) and the energy of the investigated emission ($\lambda = 3$ μ) were measured with an IEK-1 calorimeter. The spectral composition of the emission was analyzed with an IKM-1 monochromator and a GeAu crystal at liquid nitrogen temperature.

In the experiment an exact measurement was made of the quantum yield of generation, i.e., the number of stimulated emission photons relative to the absorbed $\lambda = 3470$ Å photons[1,2]. When the reaction in the mix-
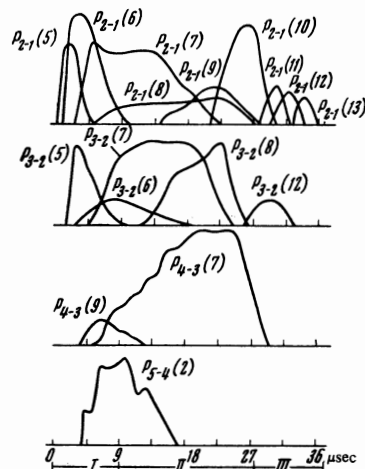

FIG. 3. Spectral decomposition of generation pulse ($\tau_p \sim 8$ μsec).

ture is initiated by means of pulsed lamps or discharges the quantum yield measurement encounters a number of difficulties stemming from the energy absorption measurement. The experiments were performed at the total mixture pressure of 40 mm Hg ($p_{H_2} = p_{F_2}$) and T = 100°K. The absorption coefficient of fluorine for $\lambda = 3470$ Å was measured and found to be 1.31×10^{-4} cm^{-1}/mm Hg. For $W_{abs} = 0.005$ J absorbed by the mixture the stimulated emission energy was $W_{ems} = 0.1$ J. Therefore $W_{ems}/W_{abs} = 20$ and the quantum yield of generation

$$W_{ems}\lambda_{ems}/ W_{abs} \lambda_{abs} = 180$$

It is noted that the quantum yield determined in this manner depends on experimental conditions; it characterizes the "chemical Q-factor" of the system or the number of reaction acts causing population inversion for the given experimental conditions.

As in the preceding experiments the duration of generation is much longer than the initiation pulse length and equals ~10 μ sec (see Fig. 5).

As the pressure of the $H_2 + F_2$ mixture increases to 100 mm Hg the energy, power, and duration of the generation pulse retain their relations observed in[1].

Figure 6 shows the time dependence of vibrational-rotational transitions $P_{2-1}(4)$ and $P_{2-1}(7)$. The simultaneous occurrence of these transitions is significantly different from the results described above (Fig. 3). This time dependence is typical of all the transitions v(3 → 1). A similar behavior is observed in transitions when reactions are initiated by a fast discharge[6].

DISCUSSION OF RESULTS

1. The use of the second harmonic of a ruby laser with the pulse length of 2.5×10^{-8} sec in fluorine photolysis makes it possible to study fast chemical reactions occurring in periods of 10^{-7} sec and less. This permitted us to study the initial stage of the generation pulse due to the reaction $F + H_2 \rightarrow HF(v = 2) + H$.

The following features are noted in the oscilloscopic traces of the $P_{2-1}(4)$ and $P_{2-1}(7)$ (Fig. 6) transition intensities. The onset of generation coincides in these transitions within the limits of measurement error of

| Transition	$\nu_{exp},$ cm^{-1}	$\nu_{theor},$ cm^{-1}	Transition	$\nu_{exp},$ cm^{-1}	$\nu_{theor},$ cm^{-1}
$P_{2-1}(3)$	3667	3666.39	$P_{3-2}(5)$	3416	3417.98
$P_{2-1}(4)$	3623	3622.61	$P_{3-2}(6)$	3375	3373.33
$P_{2-1}(5)$	3578	3577.53	$P_{3-2}(7)$	3327	3327.50
$P_{2-1}(6)$	3532	3531.21	$P_{3-2}(8)$	3281	3280.57
$P_{2-1}(7)$	3482	3483.69	$P_{3-2}(9)$	—	3232.57
$P_{2-1}(8)$	3435	3435.03	$P_{3-2}(10)$	—	3183.57
$P_{2-1}(9)$	3386	3385.29	$P_{3-2}(11)$	—	3133.62
$P_{2-1}(10)$	3335	3334.53	$P_{3-2}(12)$	3081	3082.77
$P_{2-1}(11)$	3283	3282.79	$P_{4-3}(7)$	3175	3175.22
$P_{2-1}(12)$	3231	3230.13	$P_{4-3}(8)$	3130	3129.94
$P_{2-1}(13)$	3177	3175.61	$P_{5-4}(2)$	3229	3227.63
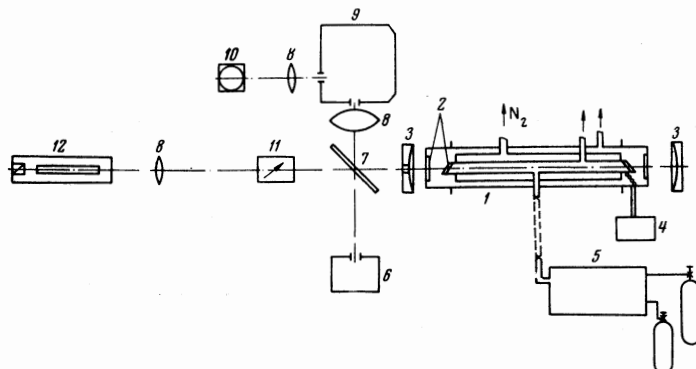
FIG. 4. Setup for ruby laser measurements. 1—cell cooled with
liquid nitrogen; 2—CaF_2 windows; 3—mirrors; 4—thermocouple; 5—gas
feed system; 6—IEK-1 calorimeter; 7—plane parallel plate; 8—lenses; 9—
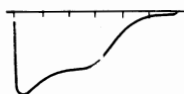IKM-1 monochromator; 10—GeAu detector; 11—KDP crystal; 12—ruby
laser.

FIG. 5. Total generation pulse for $\tau_p \sim 25$
nsec (2 μsec per division.

~ 0.02 μsec. Since these time intervals are consider-
ably shorter than the rotational relaxation time[7,8],
the rotational level distribution is determined by the
mechanism of the reaction $F + H_2$. The mixture tem-
perature at the beginning of generation rises only a
few degrees due to the energy emitted by the chemical
reaction. Furthermore, $J_{max} \sim 1$ if rotational relaxa-
tion had enough time to take place, i.e., the maximum
power would be observed at the $P_{2-1}(2)$ transition in
the generation spectrum.[1] Therefore we can be certain
that all rotational states up to $J = 10$ are filled simul-
taneously in the course of the $F + H_2$ reaction. The
strongest of all is the $J = 7$ transition due to the fact
that during photolysis fluorine atoms are generated in
a "hot" state with an energy of 0.5 ev and enter the
reaction as "hot" atoms since the cross section of the
$F + H_2$ reaction is comparable to the gas kinetic cross
section[6]. The rate of population of $v(1)$ levels is
lower than that of $v(2)$ levels: $k_2/k_1 = 3.5$[9] (k_1 and
k_2 are rate constants of populations of levels $v(1)$ and
$v(2)$; in our estimates $k_2/k_1 \sim 2.6$). Consequently a
total inversion is achieved at the start of generation[10],
the factor ensuring a simultaneous beginning of genera-
tion at the $v(2 \to 1)$ transitions.

The leading peak of generation (Fig. 6) is due to the
initial formation (by pulse photolysis) of active centers
of atomic fluorine and its subsequent reaction with
molecular hydrogen. The appearance of the second
peak in individual transitions (6) or the establishment
of a quasi-stationary regime in full generation (Fig. 5)
are due to the chain mechanism generating excited
$HF(v = 2)$ molecules because the rate constant of the
reaction $H = F_2 \to HF + F$ is an order smaller than the
rate constant of the reaction $F + H_2 \to HF + H$ and the
"next batch" of $HF(v = 2)$ molecules is formed at a

---

[1]The rotational relaxation time is of the order of 10^{-7} sec for rota-
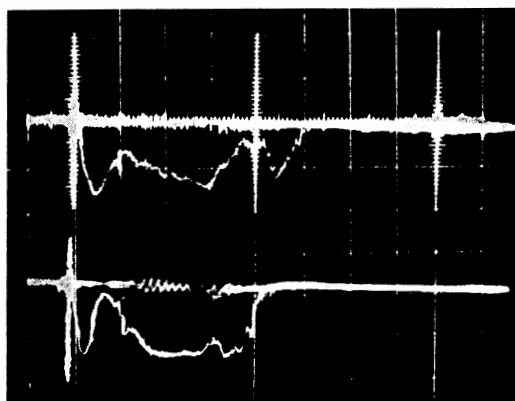tional relaxation probability of ~0.1 and p = 100 mm Hg.

FIG. 6. Oscillograms of transitions $P_{2-1}(7)$ (top) and $P_{2-1}(4)$ (bottom).
Sweep rate 0.5 μsec per division ($\tau_p \sim 25$ nsec).

lower effective rate. A complete explanation of the ob-
served processes requires the solution of a system of
kinetic equations that takes into consideration relaxa-
tion and the radiation field inside the resonator.

2. The time dependence of vibrational-rotational
transitions resulting from spectral decomposition of
a generation pulse for an 8 μsec initiation pulse, as
shown in Fig. 3, differs from the case discussed in the
preceding section by the non-simultaneous appearance
of transitions with different J. Transitions with lower
J appear first, followed by successive increase of J
from 5 to 13 for $v(2 \to 1)$, etc. This is due to different
relaxation processes taking place in the gaseous mix-
ture. Dominant are the rotational and vibrational-
rotational relaxations[10]. For molecules with a large
dipole moment such as the HF molecule the cross sec-
tions of the above-relaxation processes are large and
comparable to the gas kinetic cross section[10]. The
chemical process, always associated with a rearrange-
ment of the reacting system, has a lower probability
than the simpler process of energy redistribution[11].

Since rotational relaxation occurs in the time of
several collisions we can safely assume for a mixture
pressure of 20 mm Hg that molecular distribution
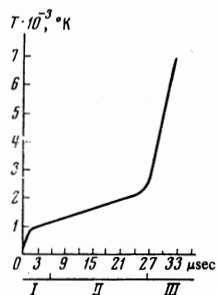among rotational levels "follows" the mixture temper-

FIG. 7. Variation of rotational temperature during generation (regions I, II, III see in Fig. 3).

ature (Fig. 3). We can use our experimental data to compute the variation of rotational temperature of HF molecules in time. Figure 7 shows the computed variation of rotational temperature during generation for an initiating pulse length of $\tau_p = 8$ μsec (adiabatic process). The rotational temperature becomes comparable toward the end of the process to the vibrational temperature and in consequence of this the generation ends[10].

3. Figure 8 shows total intensities of the transitions $\Sigma_J v_J (2 \rightarrow 1)$, line 1, and the remaining transitions $\Sigma_J v_J (n + 1 \rightarrow n)$, line 2.

The sharp peak in line 1 coincides in length with the initiating pulse length. Estimates of energy yield show that each fluorine atom generated in this interval by the reaction $F_2 + h\nu \rightarrow 2F$ enters the reaction $F + H_2 \rightarrow HF(v = 2) + H$ and emits a quantum of stimulated emission. We can thus state that the decay of free fluorine atoms in the volume is small and that the effective lifetime of fluorine is not less than 10 μsec.

4. According to Figs. 3 and 8 both reactions, $F + H_2 \rightarrow HF^* + H$ and $H + F_2 \rightarrow HF^* + F$, proceeding in the $H_2 + F_2$ mixture enable us to convert the energy liberated from the chemical reaction into stimulated emission with sufficient efficiency. Transitions $\Sigma_J v_J (2 \rightarrow 1)$ concentrate 40% of the emission energy, transitions $\Sigma_J v_J (3 \rightarrow 2)$ concentrate 30%, transitions $\Sigma_J v_J (4 \rightarrow 3)$ 22.3%, and transitions $\Sigma_J v_J (5 \rightarrow 4)$ $\sim 7.7\%$.
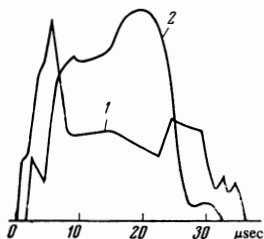

FIG. 8. Total intensities of transitions shown in Fig. 3. Line 1—vibrational-rotational band $v(2 \rightarrow 1)$; line 2—vibrational-rotational bands $v(3 \rightarrow 2) + v(4 \rightarrow 3) + v(5 \rightarrow 4)$.

5. One of the main problems concerning the generation mechanism in the $H_2 + F_2$ mixture is the role of chain branching in the formation of population inversion. The only factor that indicates branching is the weak dependence of generation power on the intensity of the initiation pulse[3,12,13]. We expect that the final answer to this problem will be given only after detailed investigation of the reaction mechanism and in such a case the use of short initiation pulses ($\sim 10^{-8}$ sec) may bring about the necessary clarity.

The authors thank Kim-Din Cher, A. A. Orlov, and M. V. Somov for help with the experiments.

[1] G. G. Dolgov-Savel'ev, V. A. Polyakov, and G. M. Chumak, Zh. Eksp. Teor. Fiz. 58, 1197 (1970) [Sov. Phys. JETP 31, 643 (1970)].

[2] V. S. Burmasov, G. G. Dolgov-Savel'ev, V. A. Polyakov, and G. M. Chumak, ZhETF Pis. Red. 10, 42 (1969) [JETP Lett. 10, 28 (1969)].

[3] N. G. Basov, L. V. Kulakov, E. P. Markin, A. I. Nikitin, and A. N. Oraevskiĭ, ZhETF Pis. Red. 9, 613 (1969) [JETP Lett. 9, 375 (1969)].

[4] O. M. Batovskiĭ, G. K. Vasil'ev, E. F. Makarov, and V. L. Tal'roze, ZhETF Pis. Red. 9, 341 (1969) [JETP Lett. 9, 200 (1969)].

[5] D. E. Mann, B. A. Thrush, D. R. Lide, Jr., J. J. Ball, and N. Acquista, J. Chem. Phys. 34, 420 (1961).

[6] G. G. Dolgov-Savel'ev and A. A. Podyminogin, Opt. Spektrosk. 1971 (in press).

[7] F. J. Zeleznik, J. Chem. Phys. 47, 3410 (1967).

[8] A. K. Barna, A. Manna, and P. Mukhopadhyay, J. Chem. Phys. 49, 2422 (1968).

[9] J. C. Polanyi and P. C. Tardy, J. Chem. Phys. 12, 5717 (1969).

[10] M. S. Dzhidzhoev, V. G. Platonenko, and R. V. Khokhlov, Usp. Fiz. Nauk 100, 641 (1970) [Sov. Phys.-Usp. 13, 247 (1960)].

[11] V. N. Kondrat'ev, Kinetika khimicheskikh gazovykh reaktsii (Kinetics of Chemical Gaseous Reactions), AN SSSR, 1958.

[12] V. L. Tal'roze, G. K. Vasil'ev, and O. M. Batovskiĭ, Kinetika i Kataliz 11, 277 (1970).

[13] G. G. Dolgov-Savel'ev, V. A. Polyakov, and G. M. Chumak, Mezhdunarodnyi simpozium po khimicheskim kvantovym generatoram Tezisy dokladov, (International Symposium on Chemical Lasers, Abstracts of Papers), Moscow, 1969, p. 6.

Translated by S. Kassel
6